12WCEE 2000

0128

INVESTIGATION OF LIQUEFIED SITE OF CHIGU, TAINAN, TAIWAN

Ni SHENG-HUOO[1] And Cheng SHIH-NAN[2]

SUMMARY

The purpose of this paper is to present the geotechnical investigation results of a case of liquefaction site during earthquake. The site is located at Chigu, Tainan, Taiwan. The earthquake is scaled as Richter Magnitude of 5.9 and occurred on March 12, 1991. Many areas of free field were liquefied but caused no much damage during the earthquake. However, a serious damage happen at harbor structure induced by liquefaction. The paper presents the case of this earthquake with the view point of geotechnical engineering. The main focus in this paper is on the reasons of why the soil liquefied during this earthquake. A total of five boreholes were drilled to investigate the soil properties of the liquefied area. Both the dynamic triaxial test and resonant column test were performed with undisturbed samples in the laboratory while the in-situ seismic downhole tests were performed in the field. The soil profiles show that both SPT-N value and shear wave velocity is low at shallow depth. The ground water level is high (less then 0.5 m below ground surface) in the coastal area. The results of liquefaction potential analysis show that the soil liquefaction in this area is positive during this earthquake.

INTRODUCTION

Taiwan is located in the seismic zone of the western pacific earthquake belt. It is often troubled by frequency earthquake, which causes great losses of lives and properties. Taiwan has its special geology with steep mountains, short streams and weak geological formation. The most important seismic hazards in Taiwan are ground shaking, structural damage or collapse, landslides and liquefaction. As shown in Figure 1, the main island of Taiwan is spindle-shaped, with the longitudinal axis extending roughly north-south for a length of 385 kilometers. The maximum width is 143 kilometers. The island occupies a total area of 35,960 square kilometers. The main island is surrounded with other fourteen subordinate islands.

The Central Range forms the backbone ridge and is the main water divide between the eastern and the western slopes of Taiwan. It bisects Taiwan island into two unequal parts, the western flank being about twice as wide as the eastern flank. Consequently the stream gradients are much steeper on the east of the Central Range. The Central Range trends northerly for a length of 350 kilometers.

The Central Range slope westward into strips of foothills and then into broad, elevated tablelands and uplifted terraces. A wide extent of coastal plain is developed on the southwest of this foothills region, bordering the Taiwan Strait on the east. This coastal plain has a north-south length of 240 km and a maximum east-west width of 45 kilometers. It is the largest coastal plain in Taiwan. The plain is covered with Alluvial deposit of clay, silt, sand, and boulders. However, the soil deposits are consists mainly of silt, and sandy soils in the shallow depth in the plain. Therefore, soil liquefaction during EQ in the plains is probably the mainly seismic hazard. Earthquakes occur almost continuously around the Taiwan island. However, only very small percentage of Earthquakes is large enough to cause noticeable damage and to be considered as major Earthquakes. Throughout recorded history, the significant historical Earthquakes induced liquefaction of soils in Taiwan is listed in Table 1. As shown in the table, the most recent Earthquake induced soil liquefied is the Tainan Earthquake. Many cases of soil liquefaction are shown in the table for the past Earthquake. However, the soil investigation in the site of soil liquefied is seldomly done before in this country. The case of the soil liquefaction in Chigu area during the Tainan Earthquake is then become interesting for the study. The main purpose of this paper is to present the results of soil investigations of the liquefied site in Chigu area during Tainan Earthquake in 1991.

[1] *Department of Civil Engineering, National Cheng-Kung University, Tainan, Taiwan E-mail: tonyni@mail.ncku.edu.tw*
[2] *Institute of Earth Sciences, Academia Sinica, P.O. Box 1-55, Nankang, Taipei, Taiwan E-mail: snan@earth.sinica.edu.tw*

Table 1 Significant Historical Earthquakes Induced Liquefaction in Taiwan

Date	Earthquake Name	Epicenter Location	Magnitude	Epicentric distance, km	Liquefaction phenomena
Nov., 1904	Chiayi EQ	(120.3° E, 23.5° N)	6.5	≈20	sand boils
March, 1906	Chiayi EQ	(120.5° E, 23.6° N)	5.8	≈10	sand boils, mud boils
April, 1906	Baiho EQ	(120.4° E, 23.4° N)	6.5	≈5	sand boils
Aug., 1927	Hsinyin EQ	(120.3° E, 23.3° N)	6.5	≈20	sand boils
Dec., 1930	Hsinyin EQ	(120.4° E, 23.3° N)	6.5	≈30	sand boils
April, 1935	Miaoli EQ	(120.8° E, 24.3° N)	7.1	≈30	mud boils
July, 1935	Miaoli EQ	(120.7° E, 24.6° N)	6.2	≈20 ≈25	settlement, landslides
Dec., 1941	Chiayi EQ	(120.5° E, 23.4° N)	7.1	≈23	landslides
Oct., 1951	Hualien EQ	(121.8° E, 24.1° N)	7.1	≈30	settlement
Nov., 1951	Taitung EQ	(120.9° E, 23.0° N)	7.3	≈30	subgrade settlement
Sept., 1959	Henchun EQ	(121.2° E, 22.1° N)	6.8	≈67	mud boils
Jan., 1964	Chianan EQ	(120.6° E, 23.2° N)	6.5	≈60	sand boils
Nov., 1986	Ilan EQ	(121.9° E, 24.2° N)	6.8	≈10	sand boils
March, 1991	Tainan EQ	(120.3° E, 23.2° N)	5.9	≈25	sand boils, mud boils

THE TAINAN EARTHQUAKE OF 1991 AND OUTLINE OF DAMAGE

The Tainan Earthquake occurred in Tainan, Taiwan at 2:04:08 PM, March 12, 1991. The epicenter position is located at 23.17° N, 120.24° E. The epicenter is approximately located Chigu and Jianjiun area with the distance from Tainan city about 26 kilometers in the northern direction. The hypocentric distance (or focus depth) is about 4.9 kilometers. The earthquake is scaled to 5.9 in Richter scale. As shown in Figure 2, the epicenters of the main shock and aftershocks are scattered within an area of approximately 50-km radius. The shocks are mostly occurred around the Chigu area. The magnitude of adjacent Tainan city is scaled to 5 while the magnitude of Chiayi is scaled to 3. The seismic damage to the ground and earth structures is mainly caused by soil liquefaction during the earthquake. The major damage includes the followings.

1. Liquefaction of level sandy ground

Sand boils was observed at a number of places in the Chigu area, expecially in free field. As shown in Figure 3, the sand boils occurred in a big dried fishing pool. Actually, there are many sand boil holes in the same pool. Many sand boils holes were also observed under water in the salt field. The foundation soils of both fishing pool and salts field are involved very loose saturated sandy soils.

2. Damage of harbour structures

There are two fishing harbours in the Chigu area. They are Masago harbour and Chinshan harbour. The earthquake caused considerable damage to the existing two harbours. Part of ground surface of levee area was collapsed due to underground soil liquefied. As shown in Figure 4(a), soils flowed out during soil liquefaction such that the concrete slab collapse due to the loss of support of soils in the Chinshan harbour area. Also, as shown in Figure 4(b), the levee of Masago harbour was subjected to about 5 to 200 mm wide crackings with 20mm to 250mm settlements.

3. Damage to highway embankment

Many highway embankments in the Chigu area were seen with slope failure. The failure frequently occurred at junctions between bridge and road. The material used for the embankments is mostly alluvial sandy soils. The foundation soils are always saturated at the junction of bridge. The slope failure may mainly caused by soil liquefaction of foundation soils of the embankment during the earthquake. In addition to slope failure of embankments, some places of country roads were seriously damage with cracking due to differential settlements, as shown in Figure 5.

4. Damage to buildings

Fortunately, There have no many buildings of three or up stories in the Chigu area. The main damage in buildings is old brick walls fall down and new cracks developing in some of old houses. Also some of the gateway of temple were seriously damage or fall down. No people dead or wounded seriously was reported in this earthquake.

SOIL INVESTIGATION IN THE CHIGU AREA

As described above, most damage were due to soil liquefied during earthquake in this area. It is interesting to know the reason why the liquefaction so easy to happen in this area during earthquake with magnitude of 5.9 only. To solve this problem, a series of geotechnical testing program were planed and performed. A total of five boreholes with the depth of 30 meters were drilled over this area. The standard penetration test (SPT) was performed every 1.5 meter and several undisturbed soil tubes were sampled at selected depths during the soil boring .

The specimen taken from split-spoon sampler is used to perform soil physical property tests. The results show that the soils with an average specific gravity of 2.69. The void ratio is ranged from 0.52 to 0.73. The moist unit weight is about 19.7 kN/m^3. The mean diameter (D_{50}) is ranged from 0.11mm to 0.18mm. Fines contents of the soil are ranged from 20% to 40%. Most of sandy soils are contained a significant fine materials. The soil profiles for the five boreholes, which are named as A1 to A5, are shown in Figure 6. As shown in the profile, the soil deposits are mainly consists of the soil classifies as SM and ML, and with some relatively thin layers of containing a significant fine materials, clay (CL). The boring results show that the soil profile is mainly formed by gray silty sand (SM) and silty clay (ML) with a relatively thin layer of clayey soil (CL) at near the top of soil deposit. The ground water level is located less than 0.5 meter. The SPT-N value is varried from 16 to more than 30 counts at the depth greater than 10 meters. However, the SPT-N value is less than 5 counts for the depth less than 3.5 meters. The typical grain size distribution curve is shown in Figure 7.

DYNAMIC SOIL PROPERTIES

Both the dynamic triaxial test and resonant column test were performed with undisturbed samples in the laboratory while the in-situ seismic downhole tests were performed in the field.

1. Dynamic triaxial test

Cyclic triaxial compression tests on the specimens were performed without drainage by CKC automatically cyclic triaxial compression test system. All specimens were initially subjected by applying the isotropic consolidated pressure under an appropriate effective confining pressure for two hours. After isotropic consolidation, specimens deformation an axial deviatoric stress is applied through a vertical ram to specimen. Computer programmed electric signal and magnitude of loading was applied by an electro-pneumatic transducer, which was controlled by pneumatic amplifiers for the application of load. An appropriate cyclic deviatoric stress without drainage was applied with a sine wave pulse at a low frequency of 1 Hz. During each test, cyclic load, axial strain and pore water pressure were continuously monitored with electronic transducers and recorded by PC computer.

The results of cyclic triaxial undrained compression tests on specimens taken from five boreholes were stated in Figure 8. The test results show that the relationship of cyclic stress ratio via the numbers of cyclic cycles to cause initial liquefaction for each specimens. It is indicated that the increase of the numbers of cyclic cycles to cause the increase of the pore water pressure, if the pore water pressure rise up to the confining pressure indicating that the effective stress momentarily dropped to zero. Based on Seed [5], this constitutes the initial liquefaction.

2. Resonant column test

Resonant column equipment used in this test series is of the fixed-free type, which is designed by Professor Stokoe in the University of Texas at Austin [2]. In this configuration, the bottom of the soil specimen is rigidly fixed to the base while the top (free end) is connected to a drive system that is used to vibrate the specimen in torsional motion. The soil specimen has the solid shape of a right circular cylinder. The basic operational principle is to excite the cylindrical specimen in the first-mode torsional motion. Once the first mode is established, measurements are made of the resonant frequency, amplitude of vibration and free-vibration-decay curve. These measurements are then combined with equipment characteristics and specimen size ton calculate shear wave velocity, shear modulus, and shearing strain amplitude using elastic theory. Material damping ratio is calculated from measurement of the free-vibration-decay curve.

By using the wave equation, the basic data-reduction equation can be expressed as:

$$\frac{I}{I_0} = \frac{\omega l}{V_s} \tan\left[\frac{\omega l}{V_s}\right]$$

in which I = mass moment of inertia of soil specimen, I_0 = mass moment of inertia of drive plate, ω = resonant circular frequency, l = length of the specimen, and V_s = shear wave velocity. From the above equation the shear modulus can be calculated as:

$$G = \rho \times V_s^2$$

in which ρ = mass density of the soil.

By assuming a viscous material damping in shear, the material damping is calculated from a decay of free vibration. Because the shearing strain varies within the specimen, an equivalent shearing strain, which is located at 2/3 of radius for solid specimen, is used to represent the average shearing strain in the specimen. All the testings and calculations are auto-controlled with microcomputer.

3. In-situ seismic downhole test

The downhole seismic method is a widely used method of evaluating in situ wave velocity profiles at geotechnical sites. With this method, the source is placed on the ground surface and receivers are placed down a single borehole. The source is then transiently excited; vertically for compression waves or horizontally for shear waves. Wave velocities are determined by evaluating travel times between the source and receivers (termed direct measurements). These conventional methods of determining wave velocities are very simple and generally result in rather smooth velocity profiles.

The test result of shear wave profiles for boreholes A2 and A4 are shown in Figure 9. As shown in Figure 9, shear wave velocity is ranged from 104 m/sec to 292 m/sec. The results show that low shear wave velocity is located at the top layer. The velocity obtained from the resonant column test is also shown in Figure 9 with a black dot point. It can be seen that the shear wave velocities obtained from both methods agree well.

EVALUATION OF SOIL LIQUEFACTION POTENTIAL

At present, many methods are available to evaluate the soil liquefaction potential for a given site. The methods used in this paper include laboratory test approach and in-situ SPT-N value method. Many SPT-N methods have been developed and adopted as the most fundamental methods in practice. In order to realize the differences between various methods, three SPT-N methods will be compared herein. The three SPT-N methods are recommended by Seed[1,7,8], JRA[3] and Tokimatsu and Yoshimi[6], respectively. Data obtained from the five boreholes plotted in the chart with the criteria recommended by seed is shown in Figure 10. As seen in the Figure, the soil located in the borehole A4 will be liquefied during the Tainan earthquake.

The results of dynamic triaxial tests related with the SPT-N methods are presented in Figure 11. It is difficult to judge which method is better than others in the figure due to the data scattering at this moment in this case. However, Seed's method seems to be better than the other two methods (Seed's correlation coefficient (R^2) is 0.2 while the others are 0.09 and 0.08) by using linear regression approach.

The equations obtained from the linear regression approach are:

Seed's method: $(\sigma_d / 2\sigma'_c) = 0.069 \left(\frac{\tau}{\sigma'_v} \right)_R + 0.28, \quad R^2 = 0.20$

JRA's method : $(\sigma_d / 2\sigma'_c) = 0.086 \left(\frac{\tau}{\sigma'_v} \right)_R + 0.28, \quad R^2 = 0.09$

T and Y's method: $(\sigma_d / 2\sigma'_c) = 0.026 \left(\frac{\tau}{\sigma'_v} \right)_R + 0.29, \quad R^2 = 0.08$

CONCLUSIONS

The liquefied area of soils at Chigu during Tainan earthquake was widely investigated. The soil profiles show that the soil deposits are mainly consists of silty sand (SM) and silty clay (ML). The SPT-N values shown in the profiles are ranged from 2 to 5 counts at the upper 3.5 m depth. The loose upper soil layer associated with high water table level creates a very good basic environment for soil liquefaction during the Tainan earthquake.

The further dynamic soil test results show that the shear wave velocity in the upper layer is low. The dynamic soil test results plot in the chart with criteria suggested by Seed show that some locations would be liquefied in this earthquake. The results from the comparison of dynamic triaxial test with the three SPT-N methods used in this paper does not strongly tell the differences in accuracy among them in this case.

ACKNOWLEDGMENTS

The authors are grateful to Mr. S. Y. Lin for his assistance in reducing data and drawing some charts. The study on which this paper is based was supported by National Science council of the Republic of China (Taiwan) through the Grunt No. NSC88-2218-E006-019. This financial support is greatly appreciated.

REFERENCES

1. Committee on Earthquake Engineering (1985), *Liquefaction of Soil During Earthquake*, NRC Report No. CETS-EE-001, 240p.
2. Isenhower, W.M. (1979), "Torsional Simple Shear/Resonant Column Properties of San Francisco Bay Mud," Geotechnical Engineering Thesis GT80-1, Civil Engineering Department, University of Texas at Austin, Austin, TX, Dec., 307 p.
3. Japan Road Association (1990), Specification for Highway Bridges-Part V: Earthquake Resistant Design. Tokyo: Japan Road Association.
4. Ni, S. H., Jan, W. T. and Juang M. R. (1997), "Evaluation of Soil Dynamic Properties in Tainan Chigu Industrial Area," Proceedings of 7th Conf. on Current Researches in Geot. Engrg., Vol. I, Aug., pp 273-280.
5. Seed, H. B. and Lee, K. L. (1966). "Liquefaction of Saturated Sand During Cyclic Loading," J. Soil Mech. Found Div., ASCE, Vol. 92, No. SM6, pp. 105-134.
6. Tokimatsu, K. and Yoshimi, Y. (1983) "Empirical Correlation of Soil Liquefaction Based on SPT-N Value and Fines Content," Soils and Foundations, Vol. 23, No. 4, Dec., pp. 56-74.
7. Seed, H. B., Idriss, I. M., and Arango, I. (1983). "Evaluation of Liquefaction Using Field Performance Data," Journal of Geotechnical Engineering, ASCE, Vol. 102, GT4, pp 246-270.
8. Seed, H. B., Tokimatsu, K., Harder, L. F, and Chung, R. M. (1984), "The Influence of SPT Procedure in Soil Liquefaction Resistance Evaluation," EERC-84/15, U. C. Berkeley, California, October.

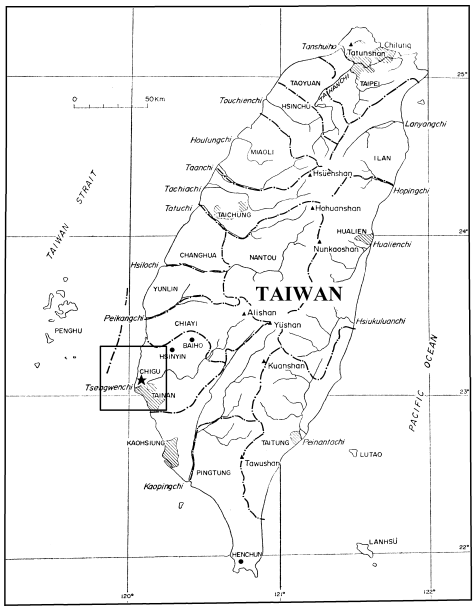

Fig. 1 Map of Taiwan

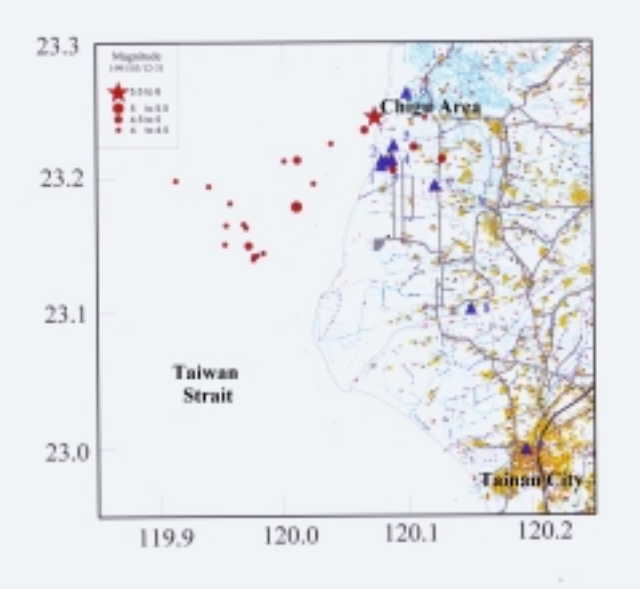

Fig. 2 Seismic intensities in the Chigu area

Fig. 4 Damage in Masago harbour

Fig. 4 Damage in Masago harbour

Fig. 3 Sand boils in dried fishing pool road

Fig. 5 Cracks damage on country

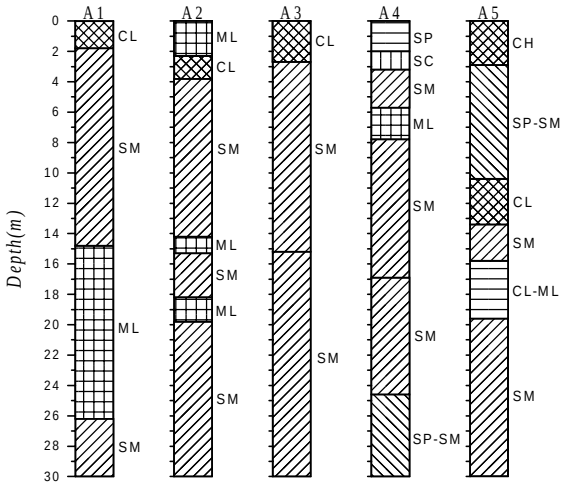

Fig. 6(a) Soil profiles of the five borecholes

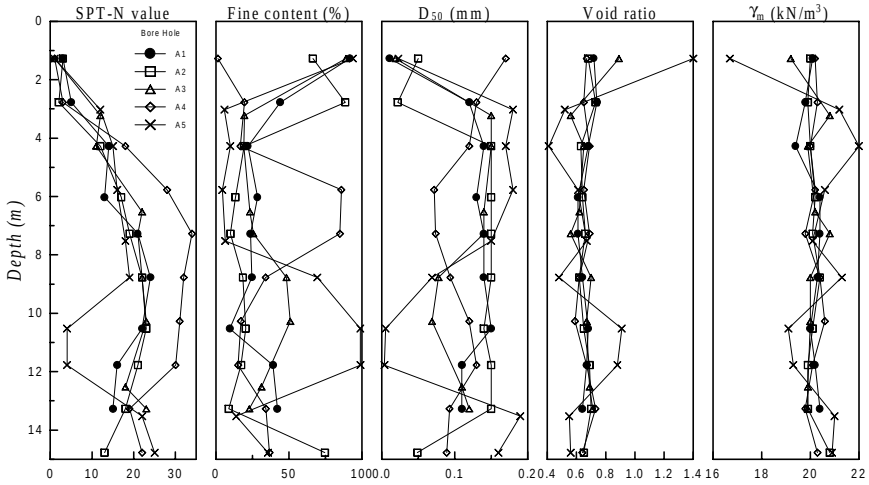

Fig. 6(b) Soil properties of the five boreholes

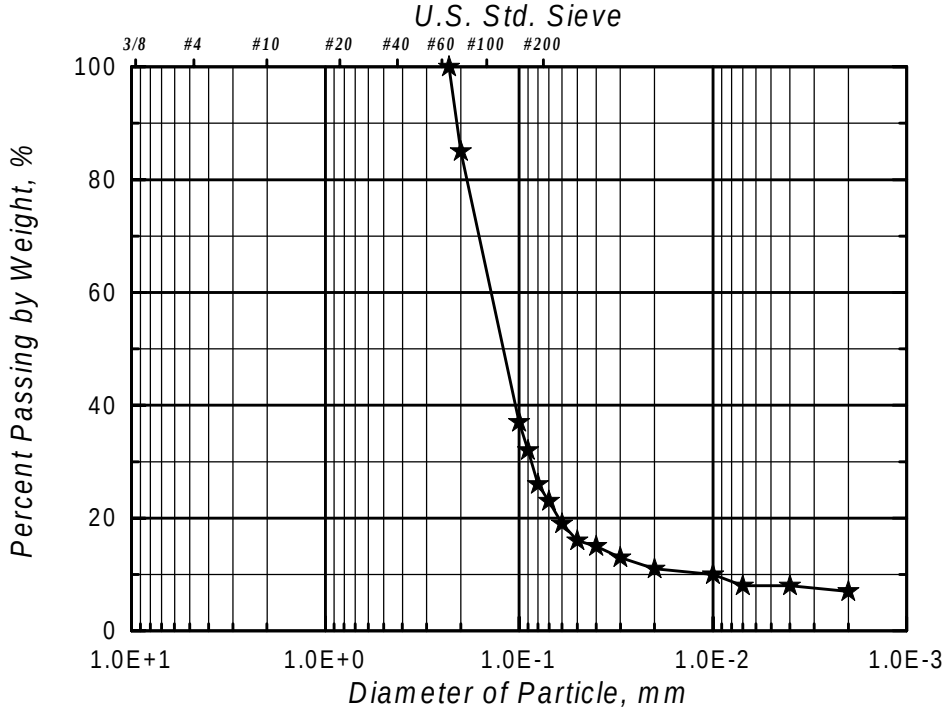

Fig. 7 Typical grain size distribution curve in Chigu soils

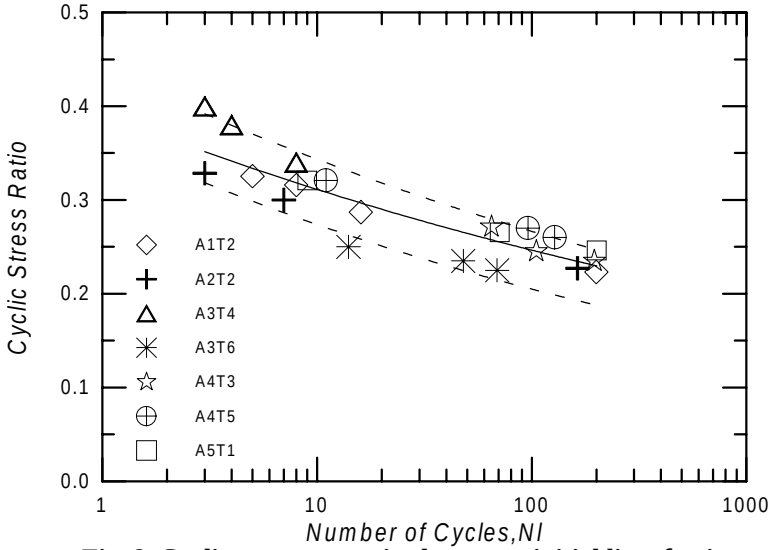

Fig. 8 Cyclic stresses required to cause initial liquefaction

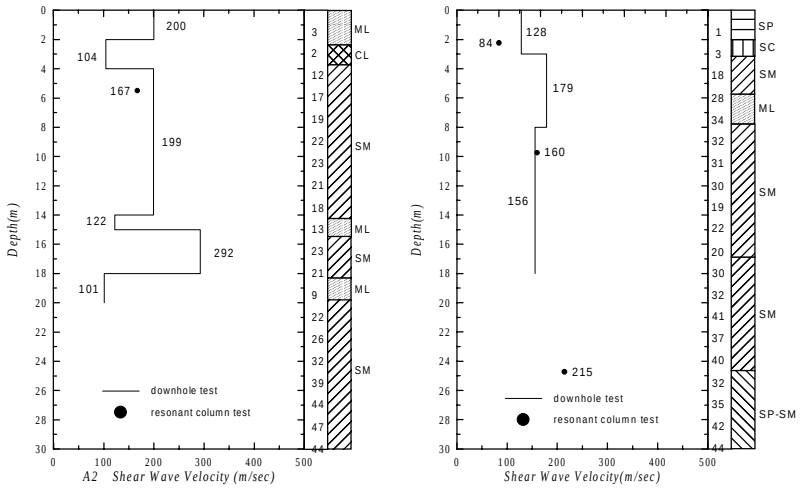

Fig. 9 Shear wave profiles of borehole A2 and A4

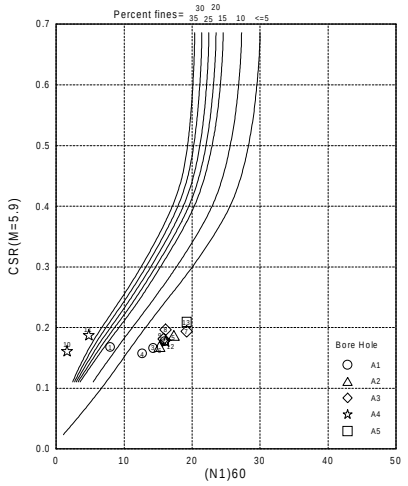

Fig. 10 Relationship between cyclic stress ratio

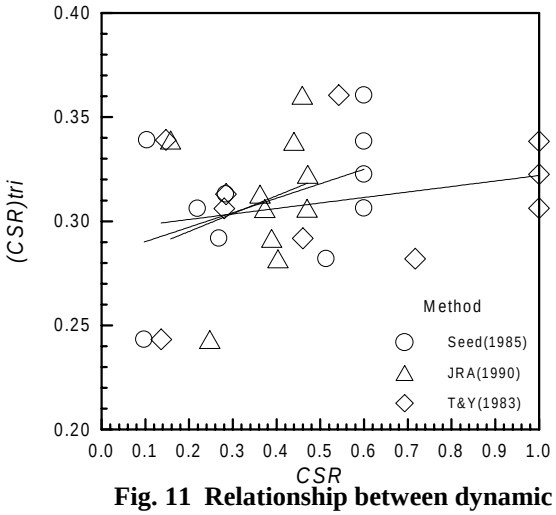

Fig. 11 Relationship between dynamic triaxial test and SPT-N method causing liquefaction and $(N_1)_{60}$ in M=5.9